

Gradient-based Trajectory Optimization with Parallelized Differentiable Traffic Simulation

Sanghyun Son^{*1}, Laura Zheng^{*1}, Brian Clipp², Connor Greenwell², Sujin Philip², and Ming C. Lin¹

Abstract—We present a *parallelized differentiable traffic simulator* based on the Intelligent Driver Model (IDM), a car-following framework that incorporates driver behavior as key variables. Our simulator efficiently models vehicle motion, generating trajectories that can be supervised to fit real-world data. By leveraging its differentiable nature, IDM parameters are optimized using gradient-based methods. With the capability to simulate up to 2 million vehicles in real time, the system is scalable for large-scale trajectory optimization. We show that we can use the simulator to filter noise in the input trajectories (*trajectory filtering*), reconstruct dense trajectories from sparse ones (*trajectory reconstruction*), and predict future trajectories (*trajectory prediction*), with all generated trajectories adhering to physical laws. We validate our simulator and algorithm on several datasets including NGSIM and Waymo Open Dataset.

I. INTRODUCTION

For design, prototyping, testing, and evaluation of dynamical systems, we often rely on computer simulations that replicate reality, such as urban dynamics or natural phenomena. Traffic simulation, for example, is often used to optimize traffic light policies [1], [2] or to train autonomous vehicles in varied scenarios [3], [4]. Traffic models come in different scales, in this paper we focus on microscopic models that simulate the movement of *every individual vehicle* [5]–[12], as opposed to macroscopic models that simulate *aggregate traffic flow* [13]–[18]. We adopt the Intelligent Driver Model (IDM) [12], an ODE describing car-following behavior, as it is widely used in diverse traffic simulators [3], [19]–[21].

When developing a traffic simulator, we aim for both efficiency and differentiability. The simulator must be efficient to gather enough data to solve the problem without excessive cost. This is especially important as traffic problems continue to grow in scale [1], [22]. Optimization techniques are also key, and they can be classified as either *gradient-based* or *gradient-free*. Among them, gradient-free methods typically require significantly more data, because of its inferior sample efficiency. To ensure sample efficiency and reduce costs in training, testing, and evaluation, we designed our simulator to be *differentiable* via auto-differentiation frameworks.

Differentiable simulation has successfully bridged real-world dynamical systems with the power of deep learning [23]–[28]. It allows a state at one timestep to be differentiable with respect to that of the previous one, enabling gradient-based optimization techniques that require

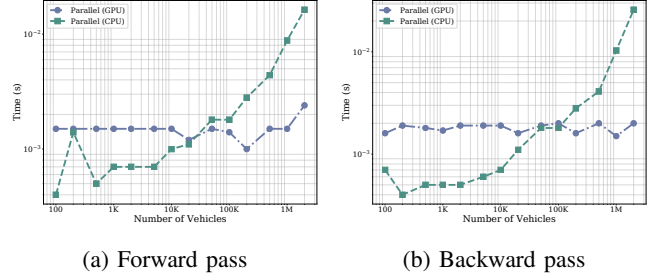


Fig. 1: **Computational cost of our traffic simulator.** Using either (multi-threaded) CPU or GPU, our simulation takes less than 30 milliseconds *per timestep* to process 2 million vehicles in both (a) forward and (b) backward pass.

fewer samples than gradient-free methods. The differentiable programming paradigm for traffic modeling has gained traction recently [2], [29]–[31], including data-driven approaches [32]. However, these methods often suffer from computational inefficiencies such as sequential processing and non-differentiable logic, limiting their practicality for real-time autonomous systems.

To address these limitations, we propose a *parallelized differentiable traffic simulator* that achieves both efficiency and differentiability. Our implementation supports both CPU and GPU parallelization and can simulate up to 2 million vehicles in real-time (Figure 1). We also introduce several differentiable modifications to the original IDM to eliminate unrealistic vehicle behaviors (e.g., backward motion), which were not addressed in previous work [2], [29]. This simulator can handle various trajectory optimization tasks, including filtering, reconstruction, and prediction (Figure 2). Specifically, in trajectory prediction, we explicitly incorporate road network and lane membership information, which existing frameworks have not done. Our main contributions are summarized as follows:

- We present an efficient traffic simulator based on IDM, which can simulate up to 2 million vehicles in real time using either *CPU or GPU parallelization*.
- We derive and implement a *differentiable IDM* layer that is guaranteed to generate realistic vehicle motions. Using the gradients from this layer, we can leverage sample-efficient gradient-based optimization schemes for traffic optimization problems.
- We validate our method by solving *large-scale trajectory filtering, reconstruction, and prediction* for autonomous driving on various datasets. Our trajectories are guaranteed to follow the physical laws, while the existing methods may not always do.

^{*}Equal contribution

¹The authors are with (1) Department of Computer Science, University of Maryland at College Park, MD, U.S.A., (2) Kitware. E-mail: {shh1295,lyzheng,lin@umd.edu}, {brian.clipp,connor.greenwell@kitware.com}, {philip.sujin@gmail.com}

II. RELATED WORK

A. Traffic Simulators

Most microscopic traffic simulators are based on car-following models, which describe vehicle acceleration using driver parameters like comfortable acceleration. Notable examples include the Newell Model [7], the Gipps Model [10], the Krauss Model [8], and the Intelligent Driver Model (IDM) [12]. Popular simulators such as SUMO [19], HighwayEnv [3], CARLA [20], and FLOW [4] use IDM to model vehicle movements, while others like MATSIM [33] and VISSIM [34] employ similar car-following models. IDM’s widespread use in simulators influenced our choice. However, these IDM-based simulators lack parallelization and differentiability, making them less suited for solving large-scale traffic problems.

Recent advancements in machine learning and GPU hardware have led to the development of parallelized or differentiable traffic simulators for large-scale traffic simulation and urban mobility optimization. MOSS [22] uses GPU power for city-scale traffic simulation based on IDM and MOBIL [35], but it lacks differentiability, preventing application with gradient-based optimization and deep learning. Other approaches have applied differentiable methods to traffic optimization and control [2], [29], [30], but they are not as efficient as MOSS. Data-driven simulators like Waymax [21] and GPUdrive [32] offer both GPU acceleration and differentiation but focus on replaying real-world trajectory logs from the Waymo Open Dataset (WOMD) [36], without reactive traffic behaviors. To the best of our knowledge, our simulator is the *first model-based traffic simulator that achieves both high efficiency and differentiability for optimization, learning, and control*.

B. Trajectory Optimization

We address three trajectory optimization problems: trajectory filtering, reconstruction, and prediction (Figure 2). For trajectory filtering, we assume we have dense observations (e.g., vehicle positions) that can be simply concatenated to construct a dense trajectory. However, numerical derivation on this trajectory amplifies noise, leading to physically impossible estimates of speed or acceleration [37] (Figure 5). To address this, various filtering methods have been proposed, including moving averages [38]–[40], spline smoothing [41], and wavelet analysis [37]. While this has been studied under “trajectory reconstruction,” we use the term “trajectory filtering” to differentiate it from our reconstruction task, which focuses on generating dense trajectories from sparse data points – essentially an interpolation task. Unlike previous model-free approaches, *our model-based approach is guaranteed to generate physically plausible trajectories*.

In the trajectory prediction task, many data-driven methods forecast future trajectories based on historical data and road context [42]–[47]. Current state-of-the-art methods use transformer architectures to model trajectories as sequences of positions, similar to natural language processing. However, none incorporate explicit micro-simulated dynamic states

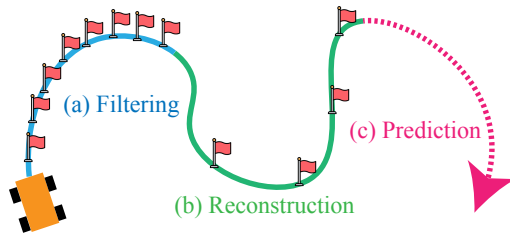


Fig. 2: **Trajectory Optimization Problems.** For the given data points (red flags), we can fit a simulated trajectory to them by optimizing IDM variables. (a) When data points are dense, we can filter physically inaccurate noises in the original trajectory. (b) When they are sparse, we can reconstruct dense trajectories. (c) We can even predict future trajectories based on the IDM variables.

into the modeling process, instead relying on highly parameterized models to implicitly capture traffic dynamics during training. This gap exists due to the lack of fast, differentiable traffic simulators—most are either sequential or non-differentiable. While some differentiable environments are used in reinforcement learning tasks [2], [28], [48], no such simulators are available for imitative or open-loop methods.

III. METHOD

A. Preliminary

Our traffic simulator is built on the Intelligent Driver Model (IDM) [12], which assumes that a vehicle’s acceleration is determined solely by its relationship to the vehicle directly ahead in the same lane. Specifically, if the position and speed of the i -th vehicle at time t are denoted as $p_i(t)$ and $v_i(t)$, and the index of its leading vehicle is $h(i)$, we compute Δp (distance gap) and Δv (speed difference) as follows:

$$\Delta p = p_{h(i)}(t) - p_i(t) - \text{length}_{h(i)}$$

$$\Delta v = v_i(t) - v_{h(i)}(t).$$

Based on these variables, we can compute the optimal spacing s_{opt} and acceleration $a_i(t)$ of the i -th vehicle as

$$s_{\text{opt}} = s_{\text{min}} + v_i(t)T_{\text{pref}} + \frac{v_i(t)\Delta v}{2\sqrt{a_{\text{max}}a_{\text{pref}}}} \quad (1)$$

$$a_i(t) = a_{\text{max}} \left[1 - \left(\frac{v_i(t)}{v_{\text{targ}}} \right)^\delta - \left(\frac{s_{\text{opt}}}{\Delta p} \right)^2 \right]. \quad (2)$$

The formulation includes several hyperparameters that describe the vehicle’s behavioral traits: a_{max} and a_{pref} for maximum and preferred acceleration, s_{min} for the minimum distance gap, T_{pref} for the preferred time to maintain current speed, and v_{targ} for the target speed. In this paper, we use meters (m) for position, meters per second (m/s) for speed, and meters per second squared (m/s²) for acceleration.

After we obtain the acceleration of each vehicle at time t , we compute its position and speed at the next time step, $t + \Delta t$ using Euler integration as follows:

$$\begin{aligned} p_i(t + \Delta t) &= p_i(t) + \Delta t \cdot v_i(t), \\ v_i(t + \Delta t) &= v_i(t) + \Delta t \cdot a_i(t). \end{aligned} \quad (3)$$

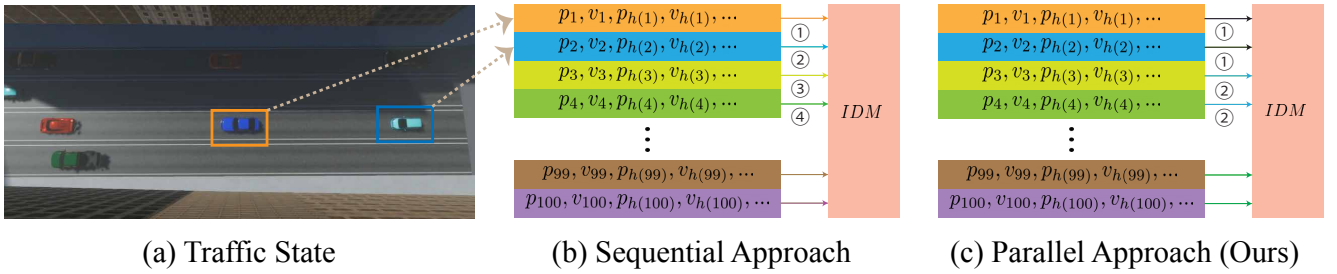


Fig. 3: **Overall Framework.** In our traffic simulator, for each frame, (a) we first collect variables for each vehicle in the scene to use in IDM. These variables include the position (p_i) and velocity (v_i) of each vehicle, and its relationship to its leading vehicle ($p_{h(i)}, v_{h(i)}$). Since we can apply IDM to each vehicle’s variables independently, we can process them in parallel, rather than sequentially. In (b) and (c), the process ordering is depicted with colors and numbers. In (c), we assume there are two computational units that can run in parallel.

The time step Δt can be adjusted depending on the scenario. While a differentiable version of this formulation has been proposed in several prior works [2], [29], these implementations often lack parallelization and result in unrealistic behaviors, such as negative speed. In the following sections, we demonstrate how to address these limitations.

B. Parallelization Scheme

Figure 3 illustrates the overall framework of our simulator. We first collect the necessary per-vehicle information for each simulation frame to compute acceleration using IDM. As shown in Figure 3(b) and (c), each vehicle’s data can be represented as independent data blocks. Due to this independence, instead of processing the blocks sequentially (Figure 3(b)), we process them in parallel (Figure 3(c)). Additionally, the IDM kernel is implemented in a differentiable manner. With this parallelization, our simulator can simulate up to 2 million vehicles in real-time on either CPU or GPU and efficiently compute gradients (Figure 1).

C. Unrealistic Behaviors

We observed that IDM often estimates negative accelerations that are physically impossible or end up with negative speed. To prevent these cases, we first set the lower bound of s_{opt} to 0, as it should be a positive value by its conceptual definition (‘optimal spacing’). Then, we set the lower bound of $a_i(t)$ to $a_{lb} = \max(-v_i(t)/\Delta t, a_{min})$, where a_{min} is a new hyperparameter that corresponds to the (physically valid) maximum deceleration. Note that we can guarantee that the next speed estimated from this acceleration term is non-negative, as we use Euler integration (Eq. 3).

To implement these lower-bound operations in a differentiable way, we use the softplus function as follows:

$$s_{opt}^* = \log(1 + \exp(s_{opt}))$$

$$a_i(t)^* = a_{lb} + \log(1 + \exp(a_i(t) - a_{lb})).$$

Note that $a_i(t)^*$ is guaranteed to exist in $[a_{min}, a_{max}]$.

IV. APPLICATION

In this section, we provide our solutions to the trajectory optimization problems using our differentiable simulator.

A. Trajectory Filtering & Reconstruction

Since the trajectory filtering and reconstruction tasks differ only in data point density, we apply the same solution to both. We assume that each trajectory is represented by a sequence of timestamps and corresponding vehicle positions in a 1-dimensional space. For the i -th trajectory, let \mathbb{T}_j^i (sec) be the j -th timestamp and \mathbb{P}_j^i (m) the corresponding vehicle position. Our goal is to generate dense trajectories that interpolate these points while adhering to physical laws. Simple linear interpolation often leads to sudden changes in estimated speed and acceleration, which are physically infeasible (Figure 5).

Therefore, we use our traffic simulator to reconstruct physically consistent trajectories that adhere to the given data as much as possible. To be specific, if we denote the temporal length of an i -th trajectory as \mathbb{T}_j^i , we simulate the motion of the ego vehicle from time 0 to \mathbb{T}_j^i , using δt as Δt in Eq. 3. Then, for each time stamp \mathbb{T}_j^i in the input, we can find the nearest time step $k_j^i \cdot \delta t$, where k_j^i is a positive integer, and compute the reconstruction loss for the i -th trajectory based on mean absolute error (MAE):

$$L_{recon}^i = \sum_{j=1}^l |\mathbb{P}_j^i - \mathbf{P}[k_j^i]|, \quad (4)$$

where \mathbf{P} is an array that stores the position of the vehicle during simulation. As our simulator supports large-scale simulation, we simulate all trajectories at once and compute the final loss $L = \sum_{i=1}^N L_{recon}^i$.

Once the reconstruction loss is computed, we minimize it using gradient-based optimization techniques. We optimize five IDM parameters ($a_{max}, a_{pref}, T_{pref}, s_{min}, v_{targ}$), which represent driver behavior and remain fixed for each trajectory. These parameters are initialized to 10, 2, 1, 5, and 50, respectively, with constraints of $[5, 10], [0.1, 5], [0.1, 5], [1, 10], [20, 60]$. We also optimize the lists of Δp_k and Δv_k for each simulation step k , initializing them to 10 and 0. Lastly, a_{min} is set to -10 and remains fixed during optimization.

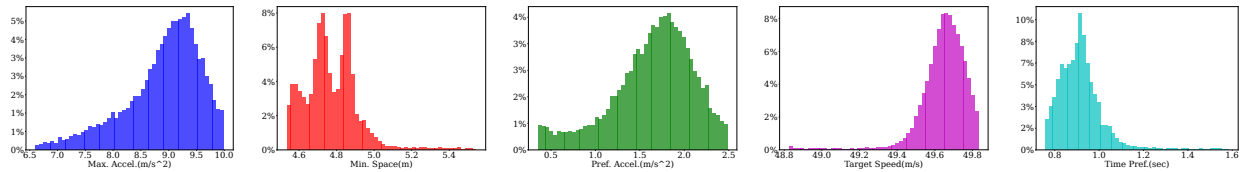


Fig. 4: **Distribution of optimized IDM parameters in trajectory reconstruction task.** Note that the distribution of each parameter adheres well to the general, real-world scenarios.

B. Trajectory Prediction

In trajectory prediction, the goal is to forecast a future trajectory based on a historical trajectory and scene context. Recent open-loop deep learning methods use neural networks to identify patterns from real-world trajectory data and predict human-like outcomes [42], [43], [47], [49]–[51]. However, common failure modes early in training involve scenarios where vehicles collide with the leading vehicle or go beyond road boundaries. Additionally, deep neural network approaches for trajectory prediction are known to be data inefficient, despite achieving SOTA results [52].

We use our differentiable traffic simulation to provide a *learning-free* performance baseline using differentiable ODE modeling and inferred road context. First, we infer traffic states from vehicle trajectories and lane shapes. For our experiments, we use the Waymo Open Motion Dataset (WOMD) [36]. Agents are assigned to lanes based on proximity to lane polyline features, and both lane polylines and agent states are projected into 1-dimensional representations for our simulator. We then fit IDM parameters using the historical trajectory, similar to the optimization process in the trajectory reconstruction task. In deep learning approaches, this information would be encoded into context embeddings. Finally, we simulate trajectories in the 1-dimensional space using the fitted IDM parameters and project them back onto the original lane polylines.

We hypothesize that by using this approach, the “predicted” trajectory will closely align with real-world trajectories, without requiring deep neural networks for learning. If successful, these ODE-based rollouts could provide a strong baseline and lower bound on performance metrics for more complex, learning-based methods.

This task is not feasible with existing simulators. While some simulators use ODE-based traffic state construction, their lack of differentiability or parallelization makes them impractical for large-scale trajectory prediction. Conversely, large-scale parallelized simulators do not explicitly construct traffic states from road data or use ODEs to model agents, making them heavily dependent on learned policies and real-world data logs for future rollouts.

V. EXPERIMENTAL RESULTS

In this section, we provide experimental results. First, we present the experimental results about the efficiency of our simulator. Then, we provide results of trajectory filtering and reconstruction tasks together and discuss those of trajectory prediction in the end. Our approach is implemented in Python and PyTorch [53]. All of our experiments were done on a

TABLE I: **Quantitative comparison for trajectory filtering & reconstruction task.** For each task, we compare the average positional error rate (Pos.), magnitude of estimated acceleration (Acc.), physically implausible trajectory rate (Imp.), and average computation time per trajectory (Time.) between compared methods. For estimated acceleration magnitude (m/s^2), we provide mean and standard variation (μ/σ).

Task	Value	Linear	MA	EMA	Spline	Ours
Fil.	Pos.↓	0.00%	0.01%	0.02%	0.00%	0.08%
	Acc.↓	6.4/5.5	0.9/0.9	0.5/0.6	3.5/2.1	0.5/0.5
	Imp.↓	100%	8.18%	4.61%	2.00%	0%
	Time.↓	0.115s	0.233s	0.237s	23.9s	0.308s
Rec.	Pos.	0.00%	0.05%	0.06%	0.01%	0.13%
	Acc.	1.8/5.4	0.5/0.7	0.2/0.4	1.6/1.9	0.3/1.1
	Imp.	99.84%	9.83%	7.24%	4.12%	0%
	Time.	0.033s	0.038s	0.042s	3.37s	0.164s

workstation equipped with Intel® Xeon® W-2255 CPU @ 3.70GHz and a single NVIDIA RTX A5000 GPU.

A. Computational Efficiency

To assess the computational efficiency of our simulator, we measured its running time for both the forward and backward passes. The total time was divided by the number of simulation steps, as running time scales proportionally with the number of steps. To evaluate scalability and device impact, we tested different numbers of vehicles using either CPU (with 16 threads) or GPU. As shown in Figure 1, our simulator can handle up to 2 million vehicles in real-time on both CPU and GPU. The CPU performs efficiently due to the use of 16 threads. For smaller numbers of vehicles, the CPU is faster since launching GPU jobs introduces overhead. However, the GPU demonstrates better scalability as the number of vehicles goes beyond 20K.

B. Trajectory Filtering & Reconstruction

1) *Dataset*: For the trajectory filtering task, we used the publicly available Next Generation Simulation (NGSIM) dataset [54], specifically 6,101 trajectories from US Highway 101, recorded every 100 milliseconds, providing dense data for filtering. For trajectory reconstruction, we used a non-public dataset containing 21,750 sparse trajectories from Singapore, recorded with a minimum sampling interval of 1 second. Each trajectory is up to 20 minutes long.

2) *Baselines*: For comparison, we used two interpolation methods (linear, spline) and two filtering techniques (moving average [38], [39], exponential moving average [40]) as baselines. For interpolation, we set δt to 0.1 and 1.0 for

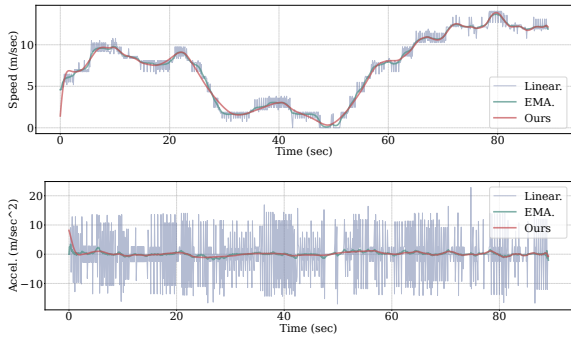


Fig. 5: **Qualitative comparison for trajectory filtering task.** For comparison, we use the speed (up) and acceleration (down) profiles for a single trajectory in the NGSIM dataset. Estimated acceleration from our method exhibits a more stable pattern than the baseline methods.

each task, estimating vehicle positions at every δt to generate dense trajectories. This matches our method, where δt is the simulation time step. For the filtering task, linear interpolation results were identical to the raw data, as the data was recorded *every* 100 milliseconds. For spline interpolation, we fitted a cubic B-spline curve using Scipy’s optimization function [55], setting bounds on the first and second derivatives (speed and acceleration) to $[0, \infty)$ and $[-10, 10]$, respectively, to ensure realistic trajectories as much as possible. For filtering, we applied both methods to the dense trajectories from linear interpolation, using a window size of 9 for moving average (MA) and a smoothing width of 5 for exponential moving average (EMA), following [39] and [40].

3) *Optimization Details:* In our optimization process, we used the Adam optimizer [56] with 500 optimization steps for both tasks. For the filtering task, we applied a constant learning rate of 0.1, while for the reconstruction task, the learning rate decayed exponentially from 0.1 to 0.01. The initial position $p(0)$ and speed $v(0)$ for each trajectory were set to 0 and $(\Delta P)/\Delta t$, where ΔP is the distance between the first two data points.

4) *Quantitative Comparison:* Table I presents quantitative results based on four criteria:

- 1) **Average positional error rate (Pos.):** Represents the precision of the trajectory, calculated by finding the nearest time step in the estimated dense trajectory for each data point, measuring the distance, dividing by the total trajectory length, and averaging across all points.
- 2) **Statistics about estimated accelerations (Acc.):** Mean and standard deviation of absolute accelerations. Lower values usually indicate more stable trajectories.
- 3) **Ratio of physically implausible trajectories (Imp.):** Ratio of trajectories with any step where absolute acceleration exceeds 10, as most real-world absolute accelerations stay below 3.
- 4) **Running Time (Time.):** Running time per trajectory.

As we can see in Table I, linear and spline interpolation achieved the best results in positional error, but most of their trajectories were physically invalid. MA and EMA

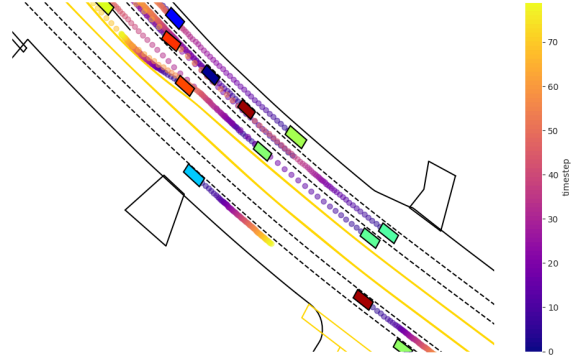


Fig. 6: **Training-free future rollouts on the Waymo Open Motion Dataset (WOMD).** We show qualitative results in trajectory forecasting with our differentiable traffic simulator. In the trajectory forecasting task, we infer the traffic state based on road graph and agent observations, including agent membership and order within lanes. Then, we fit IDM parameters for each vehicle to its 1-second historical trajectory and roll out trajectories via IDM for all agents according to their current lane. As shown above, agent vehicles maintain realistic trajectories with no deep learning or ground truth.

also performed well in positional error and gave impressive results on the second criterion. However, they still produced physically invalid trajectories, and they are not negligible—one of the trajectories exhibited an acceleration of 66, which is physically impossible. In contrast, *trajectories from our method were all physically valid, and showed stable acceleration pattern, with only a slight loss in positional error.* In terms of computational cost, our method was up to 5 times slower than simple linear interpolation *but processed each trajectory in under 0.4 seconds with parallelization.*

5) *Qualitative Comparison:* To qualitatively assess the optimized trajectories, we plot the speed and acceleration profile of a trajectory from the NGSIM dataset in Figure 5, comparing our results with linear interpolation and EMA. Linear interpolation simply mirrors the raw data (possibly with noise), so the resulting speed and acceleration profiles contain significant physically invalid noise. After applying the EMA filter, high-frequency noise is reduced, and both profiles become smoother – however, it is still not guaranteed to be physically valid. Our method produces even smoother results, and they are guaranteed to be physically valid.

6) *IDM Parameters:* As mentioned earlier, we optimize five IDM parameters during trajectory optimization. To assess the impact of optimizing these variables, we reran the trajectory reconstruction task with fixed IDM parameters. As expected, this produced worse results than our original approach: the positional error rate increased to 0.22%, and the estimated acceleration became (0.5/1.7). Optimizing the IDM parameters allows for better results by providing more flexibility. Figure 4 shows the distribution of the optimized IDM parameters, which closely aligns with real-world observations. This demonstrates that, in addition to producing better results, *our method can infer driver behavior during optimization*, offering an advantage over baseline methods.

C. A Training-Free Trajectory Forecasting Baseline

In trajectory forecasting experiments, we use our differentiable simulator to fit IDM parameters and simulate training-free trajectory rollouts on the validation set of the Waymo Open Motion Dataset (WOMD) [36], which comprises of about 15.5K 20-second segments that are further split into overlapping 9-second samples. For experiments, we evaluate the performance of training-free simulator rollouts on the WOMD validation dataset, where each sample consists of a traffic scenario centered around an autonomously driven vehicle (ADV). Similarly to the trajectory reconstruction experiments, we use the Adam optimizer to fit IDM parameters to the given 1-second trajectory histories, sampled at 10 Hz for a total of 10 timesteps. To construct the traffic state as positions along 1-dimensional lanes, we project each vehicle’s historical trajectory onto lane centers, where only vehicles within a certain distance threshold of lane centers are considered for future prediction. After solving for IDM parameters with gradient-based optimization, we initialize the traffic state to the starting state for each sample prediction and roll out 8-second futures at 10 Hz, for a total of 80 frames.

For each vehicle active in traffic lanes, we evaluate their performance with WOMD benchmark metrics. That is, we show results in mean average precision (mAP), minimum average displacement error (minADE), minimum final displacement error (minFDE), and miss rate (MissRate):

- 1) **mAP**: Mean average precision across all trajectory types and agent classes, where trajectory types include straight, straight-left, straight-right, left, right, left u-turn, right u-turn, and stationary.
- 2) **minADE**: L2 norm between closest prediction and ground truth.
- 3) **minFDE**: L2 norm between closest final position and ground truth final position.
- 4) **Miss Rate**: % of agent predictions outside of a threshold from ground truth.

Closer details on metrics can be found in Ettinger et al.’s work introducing the benchmark [36].

We show quantitative results on WOMD validation set in Table II, and compare to recent SOTA models in trajectory forecasting [45], [46], [49]–[51], [57]. In this result, we consider all benchmark trajectories and agent classes in the validation set, including that of cyclists and pedestrians in addition to vehicles.

Expectedly, results using our traffic simulator do not outperform any recent SOTA methods, and should not be directly compared against models trained on ground truth annotations. However, *we find that our simulator achieves comparable mAP performance (0.354) and acceptable distance metric performance (7.862 minADE), given no training on a large amount of pre-annotated data, where the next best mAP performance is Multipath++ [47] at 0.393.*

We interpret our simulator results as a lower-bound on trajectory forecasting performance—in other words, this is the performance produced when vehicles simply follow

TABLE II: **Waymo Open Motion Dataset validation set metric comparisons between SOTA models and training-free rollouts generated by our differentiable simulator.**

We show metric performance results generated from our simulator versus current SOTA models for trajectory prediction. Without any neural networks or training, future predictions using our simulator can attain 0.3541 mAP on validation—while this result does not outperform SOTA models, this performance is attained with *no training*, where IDM parameters are only fitted on **1-second of data**. Missing values are not reported by the respective original work.

Method	mAP↑	minADE↓	minFDE↓	MissRate↓	Params
Multipath++ [47]	0.393	0.978	2.305	0.440	-
MTR [46]	0.416	0.605	1.225	0.137	66M
ControlMTR [50]	0.422	0.590	1.201	0.132	66M
Wayformer_Ens [51]	0.430	0.530	-	-	60M
MTR++ [45]	0.435	0.591	1.199	0.130	86M
EDA [57]	0.435	0.571	1.173	0.119	-
MTRv3_Ens [49]	0.488	0.554	1.104	0.110	-
Ours	0.354	7.862	15.668	0.586	5

their personal IDM parameters according to the current road structure, with no additional information or modeling involved. We visualize an example rollout on a WOMD validation sample in Figure 6, where we show qualitatively that simulated rollouts are realistic and follow road structures.

VI. CONCLUSION

In this paper, we presented a parallelized differentiable traffic simulator based on IDM. Due to this parallelization scheme, we could simulate up to 2 million vehicles in real-time on either parallel CPU or GPU implementation. To remediate physically implausible results, we proposed modifications to the original IDM. Using this simulator, we demonstrated its capability to solve various trajectory optimization problems. For trajectory filtering and reconstruction tasks, our method efficiently estimated physically plausible trajectories without exception. Additionally, we showed that differentiable traffic simulation can be a strong training-free baseline for trajectory forecasting. The differentiability of our simulator opens up future avenues to integrate differentiable traffic simulation with deep learning for robust traffic-state-aware techniques.

A limitation of our work is that the differentiable simulation only considers vehicle modeling with IDM; this can be extended in future work to include ODE-based models of pedestrian and cyclist behavior, for more robust agent representations. Also, for trajectory filtering and reconstruction, we could come up with more complex loss functions to generate more precise trajectories. Additionally, our current implementation does not support complex road network systems. However, we believe that our simulator could be used as a core computation layer to be used in any traffic simulator in the wild that implements such systems.

Acknowledgment: This research is supported in part by Barry Mersky and Capital One E-Nnovate Endowed Professors, the ARO DURIP Grant, and the HAYSTAC Program.

REFERENCES

- [1] Z. Tang, M. Naphade, M.-Y. Liu, X. Yang, S. Birchfield, S. Wang, R. Kumar, D. Anastasiu, and J.-N. Hwang, "Cityflow: A city-scale benchmark for multi-target multi-camera vehicle tracking and re-identification," in *Proceedings of the IEEE/CVF Conference on Computer Vision and Pattern Recognition*, 2019, pp. 8797–8806.
- [2] S. Son, Y.-L. Qiao, J. Sewall, and M. C. Lin, "Differentiable hybrid traffic simulation," *ACM Transactions on Graphics (TOG)*, vol. 41, no. 6, pp. 1–10, 2022.
- [3] E. Leurent, "An environment for autonomous driving decision-making," <https://github.com/eleurent/highway-env>, 2018.
- [4] C. Wu, A. Kreidieh, K. Parvate, E. Vinitzky, and A. M. Bayen, "Flow: Architecture and benchmarking for reinforcement learning in traffic control," *arXiv preprint arXiv:1710.05465*, vol. 10, 2017.
- [5] D. C. Gazis, R. Herman, and R. B. Potts, "Car-following theory of steady-state traffic flow," *Operations research*, vol. 7, no. 4, pp. 499–505, 1959.
- [6] D. C. Gazis, R. Herman, and R. W. Rothery, "Nonlinear follow-the-leader models of traffic flow," *Operations research*, vol. 9, no. 4, pp. 545–567, 1961.
- [7] G. F. Newell, "Nonlinear effects in the dynamics of car following," *Operations research*, vol. 9, no. 2, pp. 209–229, 1961.
- [8] S. Krauss, "Microscopic modeling of traffic flow: investigation of collision free vehicle dynamics," Apr 1998.
- [9] M. Bando, K. Hasebe, A. Nakayama, A. Shibata, and Y. Sugiyama, "Dynamical model of traffic congestion and numerical simulation," *Physical review E*, vol. 51, no. 2, p. 1035, 1995.
- [10] P. G. Gipps, "A behavioural car-following model for computer simulation," *Transportation research part B: methodological*, vol. 15, no. 2, pp. 105–111, 1981.
- [11] R. Jiang, Q. Wu, and Z. Zhu, "Full velocity difference model for a car-following theory," *Physical Review E*, vol. 64, no. 1, p. 017101, 2001.
- [12] M. Treiber, A. Hennecke, and D. Helbing, "Congested traffic states in empirical observations and microscopic simulations," *Physical review E*, vol. 62, no. 2, p. 1805, 2000.
- [13] M. J. Lighthill and G. B. Whitham, "On kinematic waves ii. a theory of traffic flow on long crowded roads," *Proceedings of the royal society of london. series a. mathematical and physical sciences*, vol. 229, no. 1178, pp. 317–345, 1955.
- [14] P. I. Richards, "Shock waves on the highway," *Operations research*, vol. 4, no. 1, pp. 42–51, 1956.
- [15] H. J. Payne, "Model of freeway traffic and control," *Mathematical Model of Public System*, pp. 51–61, 1971.
- [16] G. B. Whitham, *Linear and nonlinear waves*. John Wiley & Sons, 2011.
- [17] A. Aw and M. Rascle, "Resurrection of "second order" models of traffic flow," *SIAM journal on applied mathematics*, vol. 60, no. 3, pp. 916–938, 2000.
- [18] H. M. Zhang, "A non-equilibrium traffic model devoid of gas-like behavior," *Transportation Research Part B: Methodological*, vol. 36, no. 3, pp. 275–290, 2002.
- [19] D. Krajzewicz, J. Erdmann, M. Behrisch, and L. Bieker, "Recent development and applications of sumo-simulation of urban mobility," *International journal on advances in systems and measurements*, vol. 5, no. 3&4, 2012.
- [20] A. Dosovitskiy, G. Ros, F. Codevilla, A. Lopez, and V. Koltun, "Carla: An open urban driving simulator," in *Conference on robot learning*. PMLR, 2017, pp. 1–16.
- [21] C. Gulino, J. Fu, W. Luo, G. Tucker, E. Bronstein, Y. Lu, J. Harb, X. Pan, Y. Wang, X. Chen *et al.*, "Waymax: An accelerated, data-driven simulator for large-scale autonomous driving research," *Advances in Neural Information Processing Systems*, vol. 36, 2024.
- [22] J. Zhang, W. Ao, J. Yan, C. Rong, D. Jin, W. Wu, and Y. Li, "Moss: A large-scale open microscopic traffic simulation system," *arXiv preprint arXiv:2405.12520*, 2024.
- [23] F. de Avila Belbute-Peres, K. Smith, K. Allen, J. Tenenbaum, and J. Z. Kolter, "End-to-end differentiable physics for learning and control," *Advances in neural information processing systems*, vol. 31, 2018.
- [24] J. Degraeve, M. Hermans, J. Dambre, and F. Wyffels, "A differentiable physics engine for deep learning in robotics," *Frontiers in neuro-robotics*, vol. 13, p. 6, 2019.
- [25] Y.-L. Qiao, J. Liang, V. Koltun, and M. C. Lin, "Efficient differentiable simulation of articulated bodies," in *International Conference on Machine Learning*. PMLR, 2021, pp. 8661–8671.
- [26] C. D. Freeman, E. Frey, A. Raichuk, S. Girgin, I. Mordatch, and O. Bachem, "Brax—a differentiable physics engine for large scale rigid body simulation," *arXiv preprint arXiv:2106.13281*, 2021.
- [27] J. Xu, V. Makoviychuk, Y. Narang, F. Ramos, W. Matusik, A. Garg, and M. Macklin, "Accelerated policy learning with parallel differentiable simulation," *arXiv preprint arXiv:2204.07137*, 2022.
- [28] S. Son, L. Zheng, R. Sullivan, Y.-L. Qiao, and M. Lin, "Gradient informed proximal policy optimization," *Advances in Neural Information Processing Systems*, vol. 36, 2024.
- [29] P. Andelfinger, "Differentiable agent-based simulation for gradient-guided simulation-based optimization," in *Proceedings of the 2021 ACM SIGSIM Conference on Principles of Advanced Discrete Simulation*, 2021, pp. 27–38.
- [30] A. Scibior, V. Lioutas, D. Reda, P. Bateni, and F. Wood, "Imagining the road ahead: Multi-agent trajectory prediction via differentiable simulation," in *2021 IEEE International Intelligent Transportation Systems Conference (ITSC)*, 2021, pp. 720–725.
- [31] L. Zheng, S. Son, and M. C. Lin, "Traffic-aware autonomous driving with differentiable traffic simulation," in *2023 IEEE International Conference on Robotics and Automation (ICRA)*. IEEE, 2023, pp. 3517–3523.
- [32] S. Kazemkhani, A. Pandya, D. Cornelisse, B. Shacklett, and E. Vinitzky, "Gpudrive: Data-driven, multi-agent driving simulation at 1 million fps," Aug. 2024. [Online]. Available: <http://arxiv.org/abs/2408.01584>
- [33] MATSim Association, "The multi-agent transport simulation matsim." [Online]. Available: <https://matsim.org/>
- [34] PTV Group, "Vissim: Multimodal traffic simulation software." [Online]. Available: <https://www.ptvgroup.com/en-us/products/ptv-vissim>
- [35] M. Treiber and A. Kesting, "Modeling lane-changing decisions with mobil," in *Traffic and Granular Flow '07*. Springer Berlin Heidelberg, 2009, p. 211–221.
- [36] S. Ettinger, S. Cheng, B. Caine, C. Liu, H. Zhao, S. Pradhan, Y. Chai, B. Sapp, C. R. Qi, Y. Zhou, Z. Yang, A. Chouard, P. Sun, J. Ngiam, V. Vasudevan, A. McCauley, J. Shlens, and D. Anguelov, "Large scale interactive motion forecasting for autonomous driving: The waymo open motion dataset," in *Proceedings of the IEEE/CVF International Conference on Computer Vision (ICCV)*, October 2021, pp. 9710–9719.
- [37] M. R. Fard, A. S. Mohaymany, and M. Shahri, "A new methodology for vehicle trajectory reconstruction based on wavelet analysis," *Transportation Research Part C: Emerging Technologies*, vol. 74, pp. 150–167, 2017.
- [38] A. Duret, C. Buisson, and N. Chiabaut, "Estimating individual speed-spacing relationship and assessing ability of newell's car-following model to reproduce trajectories," *Transportation research record*, vol. 2088, no. 1, pp. 188–197, 2008.
- [39] S. Ossen and S. P. Hoogendoorn, "Validity of trajectory-based calibration approach of car-following models in presence of measurement errors," *Transportation Research Record*, vol. 2088, no. 1, pp. 117–125, 2008.
- [40] C. Thiemann, M. Treiber, and A. Kesting, "Estimating acceleration and lane-changing dynamics from next generation simulation trajectory data," *Transportation Research Record*, vol. 2088, no. 1, pp. 90–101, 2008.
- [41] J. Jun, R. Guensler, and J. H. Ogle, "Smoothing methods to minimize impact of global positioning system random error on travel distance, speed, and acceleration profile estimates," *Transportation Research Record*, vol. 1972, no. 1, pp. 141–150, 2006.
- [42] A. Seff, B. Cera, D. Chen, M. Ng, A. Zhou, N. Nayakanti, K. S. Refaat, R. Al-Rfou, and B. Sapp, "Motionlm: Multi-agent motion forecasting as language modeling," 2023.
- [43] N. Nayakanti, R. Al-Rfou, A. Zhou, K. Goel, K. S. Refaat, and B. Sapp, "Wayformer: Motion forecasting via simple & efficient attention networks," in *2023 IEEE International Conference on Robotics and Automation (ICRA)*, 2023, pp. 2980–2987.
- [44] Z. Zhou, J. Wang, Y.-H. Li, and Y.-K. Huang, "Query-centric trajectory prediction," in *Proceedings of the IEEE/CVF Conference on Computer Vision and Pattern Recognition (CVPR)*, 2023.
- [45] S. Shi, L. Jiang, D. Dai, and B. Schiele, "Mtr++: Multi-agent motion prediction with symmetric scene modeling and guided intention querying," *arXiv preprint arXiv:2306.17770*, 2023.
- [46] —, "Motion transformer with global intention localization and local movement refinement," *Advances in Neural Information Processing Systems*, 2022.

- [47] B. Varadarajan, A. Hefny, A. Srivastava, K. S. Refaat, N. Nayakanti, A. Cornman, K. Chen, B. Douillard, C. P. Lam, D. Anguelov, and B. Sapp, "Multipath++: Efficient information fusion and trajectory aggregation for behavior prediction," in *2022 International Conference on Robotics and Automation (ICRA)*. IEEE Press, 2022, p. 7814–7821. [Online]. Available: <https://doi.org/10.1109/ICRA466639.2022.9812107>
- [48] Y.-L. Qiao, J. Liang, V. Koltun, and M. C. Lin, "Scalable differentiable physics for learning and control," in *ICML*, 2020.
- [49] C. Shi, S. Shi, and L. Jiang, "Mtr v3: 1st place solution for 2024 waymo open dataset challenge - motion prediction," 2024.
- [50] J. Sun, C. Yuan, S. Sun, S. Wang, Y. Han, S. Ma, Z. Huang, A. Wong, K. P. Tee, and M. H. Ang Jr, "Controlmtr: Control-guided motion transformer with scene-compliant intention points for feasible motion prediction," *arXiv preprint arXiv:2404.10295*, 2024.
- [51] S. Ettinger, K. Goel, A. Srivastava, and R. Al-Rfou, "Scaling motion forecasting models with ensemble distillation," *arXiv preprint arXiv:2404.03843*, 2024.
- [52] V. Bharilya and N. Kumar, "Machine learning for autonomous vehicle's trajectory prediction: A comprehensive survey, challenges, and future research directions," *Vehicular Communications*, p. 100733, 2024.
- [53] A. Paszke, S. Gross, F. Massa, A. Lerer, J. Bradbury, G. Chanan, T. Killeen, Z. Lin, N. Gimelshein, L. Antiga *et al.*, "Pytorch: An imperative style, high-performance deep learning library," *Advances in neural information processing systems*, vol. 32, 2019.
- [54] V. Alexiadis, J. Colyar, J. Halkias, R. Hranac, and G. McHale, "The next generation simulation program," *Institute of Transportation Engineers. ITE Journal*, vol. 74, no. 8, p. 22, 2004.
- [55] P. Virtanen, R. Gommers, T. E. Oliphant, M. Haberland, T. Reddy, D. Cournapeau, E. Burovski, P. Peterson, W. Weckesser, J. Bright *et al.*, "Scipy 1.0: fundamental algorithms for scientific computing in python," *Nature methods*, vol. 17, no. 3, pp. 261–272, 2020.
- [56] D. P. Kingma, "Adam: A method for stochastic optimization," *arXiv preprint arXiv:1412.6980*, 2014.
- [57] L. Lin, X. Lin, T. Lin, L. Huang, R. Xiong, and Y. Wang, "Eda: Evolving and distinct anchors for multimodal motion prediction," in *Proceedings of the AAAI Conference on Artificial Intelligence*, vol. 38, no. 4, 2024, pp. 3432–3440.